Available online at www.sciencedirect.com
SCIENCE DIRECT
Journal of Catalysis 237 (2006) 94–101
JOURNAL OF CATALYSIS
www.elsevier.com/locate/jcat

Gas-phase selective oxidation of alcohols: In situ electrolytic nano-silver/zeolite film/copper grid catalyst

Jiang Shen, Wei Shan, Yahong Zhang, Junming Du, Hualong Xu, Kangnian Fan, Wei Shen *, Yi Tang *

Department of Chemistry and Shanghai Key Laboratory of Molecular Catalysis and Innovative Materials, Fudan University, Shanghai 200433, People's Republic of China

Received 27 August 2005; revised 25 October 2005; accepted 26 October 2005

Available online 28 November 2005

Abstract

The selective oxidation of a series of alcohols to their corresponding carbonyl products was carried out over a rationally designed in situ electrolytic nano-silver/zeolite film/copper grid (SZF) catalyst, which was prepared by a combination of the seed-film method for the fabrication of an ultrathin zeolite film and the in situ electrolytic process for the formation of highly dispersed silver nanoparticles. At a relatively low reaction temperature (ca. 320 °C), the SZF catalyst with highly dispersed in situ electrolytic silver nanoparticles exhibited much higher activity for the oxidation of mono-alcohols and higher selectivity for ketonic aldehyde in the oxidation of di-alcohols than the conventional bulk electrolytic silver catalyst. On the basis of the combination of diffuse reflectance ultraviolet visible spectroscopy, X-ray photoelectron spectroscopy, scanning electron microscopy, transmission electron microscopy, X-ray diffraction, and thermoanalysis, the remarkably high activity and selectivity of the SZF catalyst was attributed to the highly dispersed silver nanoparticles, which were stabilized by the zeolite film against sintering, and, accordingly, a large amount of Ag^{+} ions and $Ag_n^{\delta+}$ clusters existed in the silver nanoparticles. The improvements of the catalytic performance of the SZF catalyst in a wide application extension will bring new concerns in both theoretical and applied fields.

Keywords: In situ electrolytic silver nanoparticles; Zeolite film; Alcohol; Carbonyl; Selective oxidation

1. Introduction

Selective oxidation of alcohols to carbonyls in the gas phase is one of the most important chemical transformations in industrial chemistry because of the significance of ketones and aldehydes in the syntheses of drugs, vitamins, and fragrances, as well as in many complex syntheses [1–3]. Currently the focus is on two types of reactions: the selective oxidation of mono-alcohols (Eq. (1)) [4,5], where the desired products are often those of moderate oxidation (i.e., aldehydes and ketones), and the selective oxidation of polyhydric alcohols (Eq. (2)) [1,2,6], where the target products are often moderately oxidized compounds. Products of lean oxidation (α-hydroxyketone), and overoxidation (carboxyl acid, CO_2) or cracking should be avoided. The complexity of the selective oxidation of polyhydric alcohols is due more to the catalyst design.

Up to now, several silver-based catalysts, including bulk silver and supported silver catalysts, have been developed for the oxidation of alcohols [7–10]. However, some serious problems are still encountered in the application of such catalysts. For example, in conventional bulk silver (e.g., industrial electrolytic silver), the low catalytic activity at low temperature often leads to the formation of byproducts of lean oxidation (e.g., α-hydroxyketone). In contrast, at a higher reaction temperature (>500 °C), the products of cracking and/or overoxidation are mainly obtained. Attempts have been made to improve the catalytic performance of silver-based catalysts by either adding additives to bulk silver catalysts [7] or dispersing the silver particles on suitable supports [11]. Supported silver is expected to enhance the dispersion and stability (i.e., antisintering ability) of silver, and thus also enhance its catalytic activity at relatively low temperatures. However, compared with bulk silver cata-

* Corresponding authors. Fax: +86 21 65641740.
E-mail addresses: wshen@fudan.edu.cn (W. Shen), yitang@fudan.edu.cn (Y. Tang).

0021-9517/$ – see front matter
doi:10.1016/j.jcat.2005.10.027

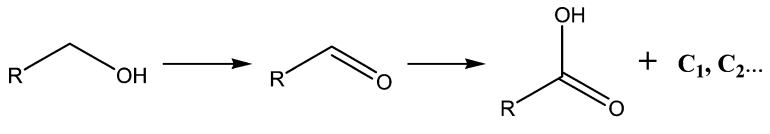

(1)

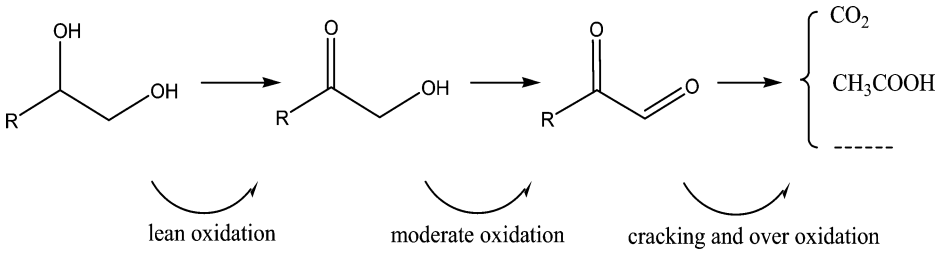

(2)

(R= H, CH_3, CH_3CH_2.....)

lysts, supported silver catalysts usually have a low heat conductivity, which greatly restricts their practical application, especially in some strongly exothermic oxidation reactions. Hence the design of a catalyst with elaborate structure and better performance remains a challenge for research on alcohol catalytic oxidation, especially those with relatively complex molecular structures (e.g., polyhydric alcohols), for which the currently available catalysts are inapplicable because of their complex selectivity and/or low activity at low temperatures. The development of a catalyst combining the advantages of both the bulk silver catalysts (e.g., conventional electrolytic silver) and the supported silver catalysts would be highly desirable for this purpose.

In our previous communication [1], we developed a novel silver-based catalyst for the selective oxidation of 1,2-propylene glycol through the in situ generation of electrolytic silver nanoparticles over an ultra-thin zeolite film precoated on a copper grid. It was suggested that the zeolite film would hinder sintering of the highly dispersed silver nanoparticles [12,13] and thereby endow the catalyst with high activity and selectivity for the selective oxidation of 1,2-propylene glycol at a relatively low temperatures. Furthermore, because of the existence of the copper grid substrate, the catalyst has a high thermal conductivity, which is beneficial to the exothermal oxidation reaction. In this paper we report an in-depth and wide-ranging investigation of the origin of the high activity of this novel nanosilver/zeolite film/copper grid (SZF) catalyst at low temperature and the possibility that excellent catalytic performance can be embodied in selective oxidation covering a wide range of alcohols with different physical and chemical features. A series of alcohols with different molecular structures and/or numbers of hydroxyl groups are used as the reactants to investigate the applicability of the SZF catalyst. The reasons for the SZF catalyst's high activity and selectivity are explored through detailed characterizations of the prepared catalyst by diffuse reflectance ultraviolet visible spectroscopy (UV–vis DRS), X-ray photoelectron spectroscopy (XPS), scanning electron microscopy (SEM), transmission electron microscopy (TEM), X-ray diffraction (XRD), and thermoanalysis.

2. Experimental

2.1. Catalyst preparation

The copper grid was coated with a thin zeolite film by a previously developed seed-film method [14]. Typically, the copper grid was first seeded with a monolayer of nanosized zeolite LTA with the aid of cationic polyelectrolytes. Then the seeded copper grid was immersed in a solution with the molar ratio of 80 Na_2O:Al_2O_3:9 SiO_2:5000 H_2O at 80 °C for 5 h to fabricate the zeolite film-coated copper (ZFC) grid. Afterwards, the ZFC grid was used as the cathode in an electrolytic cell containing 5 wt% $AgNO_3$ solution to prepare the target SZF catalyst. The electric current density of the electrolytic process was 16 A dm^{-2}, the electrolysis temperature was 55 °C, and the time was 1 min. The catalyst was finally calcined in air at 400 °C for 2 h.

For comparison, a bulk electrolytic silver catalyst was prepared by a traditional electrolytic process with silver as an anode and platinum plate as a cathode under the same conditions as the SZF catalyst.

The silver content in the SZF catalyst was determined to be 7 wt% by inductively coupled plasma-atomic emission spectrometry (ICP-AES) analysis, and the Si/Al ratio of the zeolite film was measured as 1 (the typical value of zeolite LTA) by energy-dispersive X-ray (EDX) analysis. The surface area of silver in the two catalysts was measured through the hydrogen–oxygen titration method. The surface area of the in situ electrolytic silver nanoparticles in the SZF catalyst was about 74 $m^2\,g^{-1}$, whereas that of the bulk electrolytic silver prepared by conventional process was <1 $m^2\,g^{-1}$.

2.2. Catalyst characterization

The SEM and TEM images of the catalysts were obtained on Philips XL30 and JEOL JEM-2010 instruments with acceleration voltages of 20 and 200 kV, respectively. The TG and DTA data were recorded in air atmosphere on a Perkin–Elmer 7 thermal analyzer. The XPS analysis was carried out with a

Perkin–Elmer PHI 5000C ESCA system using Al-K_α radiation (1486.6 eV) at a power of 250 W. The pass energy was set at 93.9 eV, and the binding energies were calibrated by using contaminant carbon at a BE of 284.6 eV. The UV–vis DRS spectra were recorded on a Shimadzu UV-2450 UV–vis spectrophotometer. The XRD patterns were obtained on a Bruker D8 advance diffractometer over the 2θ range from 5° to 90° with Cu-K_α radiation. The elemental analyzes were performed by ICP-AES and EDX attached in the TEM equipment.

2.3. Catalytic oxidation tests

The catalytic oxidation of alcohols was carried out in a continuous-flow, fixed-bed reactor under atmospheric pressure with oxygen as the oxidant and nitrogen as the diluent gas. The volume ratio of oxygen to nitrogen was 1:15. The molar ratio of O_2 to alcoholic hydroxyl was about 0.6. The amount of the SZF catalyst loaded in the reactor was 80 mg (volume = 0.04 ml), whereas that of the bulk electrolytic silver catalyst was 1.0 g (volume = 0.28 ml). The LHSV of reactants varied from 20 to 50 $g_{alcohol}\, g_{cat}^{-1}\, h^{-1}$ on the SZF catalyst and from 4 to 20 $g_{alcohol}\, g_{cat}^{-1}\, h^{-1}$ on the bulk electrolytic silver catalyst, respectively. The reaction temperature varied from 280 to 360 °C. The products were analyzed by on-line gas chromatography (GC) analysis.

3. Results and discussion

3.1. Catalytic behavior

3.1.1. Selective oxidation of aliphatic mono-alcohols

Table 1 shows the activities and product distributions of the oxidation of 3,5,5-trimethyl hexanol on the SZF and bulk electrolytic silver catalysts. With the decrease of the space time at 320 °C, both catalysts exhibited a decline in activity and an increase in aldehyde selectivity. However, it seems difficult to obtain a rational comparison at the same space time due to the huge difference in the activities. Therefore, we lowered the space time of the SZF catalyst (0.23 s) to about 1/7 of that of the bulk electrolytic silver (1.62 s). It is noteworthy that even at such a low space time, the SZF catalyst still exhibited much higher activity than the bulk electrolytic silver catalyst, but a similar selectivity to aldehyde (Table 1). To enhance conversion of the conventional bulk electrolytic silver catalyst, a higher reaction temperature of 500 °C was adopted. But at this temperature, a large quantity of cracking and overoxidized products was generated on the bulk electrolytic silver catalyst even though it had a higher catalytic activity. This indicates that the enhancement of low-temperature activity is more important for the partial oxidation of 3,5,5-trimethyl hexanol. With the development of fine chemistry, an increasing number of alcohols with large, complex molecular structures will be involved in industrial selective oxidation processes. Therefore, the development of partial oxidation catalysts that can operate at lower temperatures is pivotal to enhancing the yield of the partially oxidized target product.

Table 1
Conversion and product distribution of 3,5,5-trimethyl hexanol oxidation

Catalyst	Temperature (°C)	LHSV (h^{-1})	Space time (s)	Conversion (%)	Selectivity (%)	
					T.H.[a]	C.O.[b]
SZF	280	50	0.23	37	86	14
	320	20	0.58	79	64	36
		40	0.29	51	88	12
		50	0.23	43	86	14
	360	50	0.23	46	87	13
Bulk electrolytic silver	280	4	1.62	12	83	17
	320	4	1.62	17	85	15
		10	0.65	11	92	8
		20	0.32	8	94	6
	360	4	1.62	22	83	17
	500	4	1.62	49	54	46

[a] T.H. = 3,5,5-trimethyl hexanal.
[b] C.O. = cracking and over oxidation products, O_2/hydroxyl = 0.6.

Fig. 1 shows the results of some representative aliphatic monoalcohols on the SZF catalyst. Like 3,5,5-trimethyl hexanol,

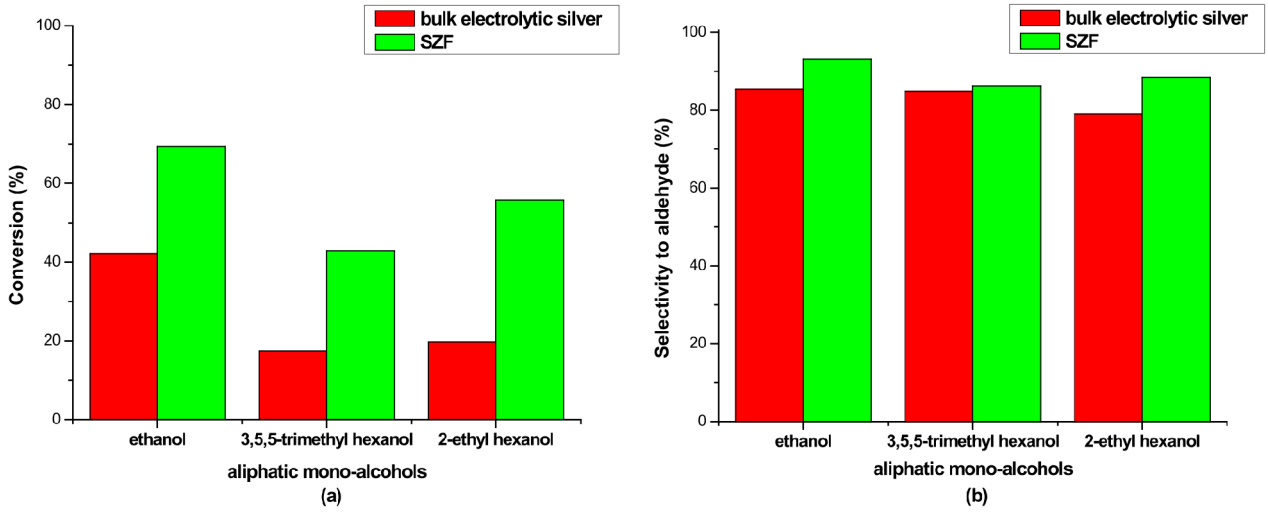

Fig. 1. Comparison of the conversion (a) and selectivity to aldehyde (b) in the selective oxidation of various acyclic mono-alcohols over the SZF and the bulk electrolytic silver catalysts at 320 °C. O_2/hydroxyl = 0.6, LHSV of the SZF catalyst = 50 h^{-1}, LHSV of the bulk electrolytic silver catalyst = 4 h^{-1}.

at a similarly high selectivity to aldehydes (Fig. 1b), all alcohols had much higher oxidation activity over the SZF catalyst than over the bulk electrolytic silver catalyst (Fig. 1a). Through a combination of a high activity and selectivity of the SZF catalyst, a high yield of the target aldehydes could be easily achieved at relatively low temperatures, while effectively avoiding the cracking and overoxidized products generated at high temperatures.

3.1.2. Selective oxidation of di-alcohols

The selective oxidation of di-alcohols is even more challenging than that of mono-alcohols, due to the existence of more than one hydroxyl group. According to Eq. (2), the production of hydroxyketone (the byproduct of lean oxidation) is the main reason for the decreased selectivity to the target products at relatively low temperatures. Table 2 gives the conversion and product distribution in the selective oxidation in 1,2-butylene glycol catalyzed by the SZF catalyst and the conventional bulk electrolytic silver catalyst between 300 and 360 °C. As in the case of mono-alcohol, the activity and selectivity of di-alcohol were also influenced by the space time, and the catalytic behavior of the SZF catalyst was still compared with bulk electrolytic silver at the space time as $<1/7$ of the latter. However, in contrast to the results for the mono-alcohols (Table 1), the SZF catalyst has a slightly higher conversion of 1,2-butylene glycol than the bulk electrolytic silver catalyst, but much higher selectivity to ethyl glyoxal, the target product of the moderate oxidation. In other words, even at $1/7$ of space time, the SZF catalyst still had the ability to produce a high yield of product with moderate oxidization, indicating that the silver species in the SZF catalyst have higher activity than those in the bulk electrolytic silver catalyst. The high activity of the SZF catalyst can also be confirmed by its relatively high yields of cracking and overoxidized byproducts at even mild reaction temperatures.

Table 2
Conversion and product distribution of 1,2-butylene glycol oxidation

Catalyst	Temperature (°C)	LHSV (h^{-1})	Space time (s)	Conversion (%)	Selectivity (%)		
					H.K.[a]	E.G.[b]	C.O.[c]
SZF	300	50	0.14	78	23	66	11
	320	20	0.35	92	7	61	32
		40	0.18	91	9	80	11
		50	0.14	88	10	77	13
	360	50	0.14	90	9	70	21
Bulk electrolytic silver	300	4	1.01	60	64	31	5
	320	4	1.01	67	58	36	6
		10	0.40	43	55	38	7
		20	0.20	29	72	24	4
	360	4	1.01	78	52	42	6

[a] H.K. = 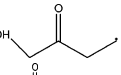

[b] E.G. = 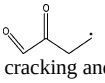

[c] C.O. = cracking and over oxidation products; O_2/hydroxyl = 0.6.

Fig. 2 illustrates the results of the conversion and selectivity to target products of three different di-alcohols catalyzed by the bulk electrolytic silver and SZF catalysts. For all di-alcohols, the SZF catalyst had a much higher selectivity to the target products as well as a slightly higher conversion than the conventional bulk electrolytic silver catalyst, demonstrating the efficiency of the SZF catalyst for the oxidation of aliphatic di-alcohols.

3.1.3. Selective oxidation of aromatic and alicyclic alcohols

Other types of alcohols, including aromatic and alicyclic alcohols, were also investigated over both types of catalysts to demonstrate the universal superiority of the SZF catalyst over the conventional bulk electrolytic silver catalyst. Table 3 lists the conversion and selectivity in the selective oxidation of cyclohexanol. It is clear that, within the selected reaction temperature range, both the activity and selectivity of the SZF catalyst were much higher than those of the bulk electrolytic silver catalyst even at a $1/7$ space time. The main byproduct over the bulk electrolytic silver was cyclohexene, the dehydration prod-

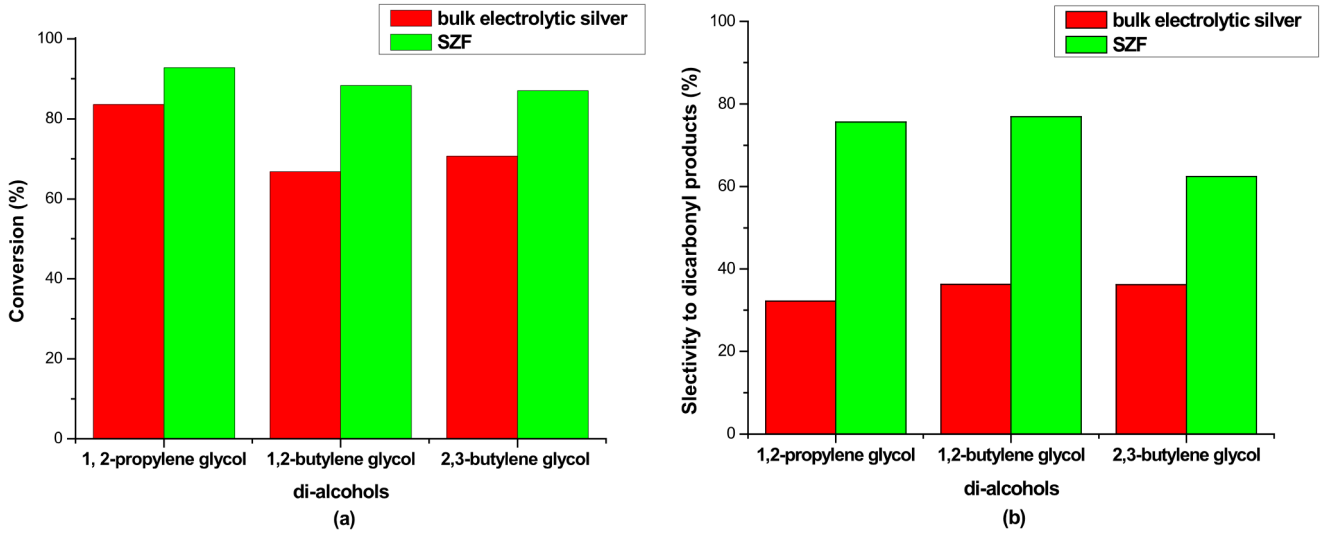

Fig. 2. Comparison of the conversion (a) and selectivity to di-carbonyl products (b) in the selective oxidation of various acyclic di-alcohols over the SZF and the bulk electrolytic silver catalysts at 320 °C. O_2/hydroxyl = 0.6, LHSV of the SZF catalyst = 50 h^{-1}, LHSV of the bulk electrolytic silver catalyst = 4 h^{-1}.

Table 3
Conversion and product distribution of cyclohexanol oxidation

Catalyst	Temperature (°C)	LHSV (h^{-1})	Space time (s)	Conversion (%)	Selectivity (%)		
					C.H.one[a]	C.H.ene[b]	C.O.[c]
SZF	300	50	0.16	22	50	40	10
	320	20	0.40	38	61	29	10
		40	0.20	29	50	37	13
		50	0.16	27	53	32	15
	360	50	0.16	40	54	30	16
Bulk electrolytic silver	300	4	1.12	10	28	63	9
	320	4	1.12	14	31	57	12
		10	0.45	10	24	68	8
		20	0.22	7	22	73	5
	360	4	1.12	25	45	41	14

[a] C.H.one = cyclohexanone.
[b] C.H.ene = cyclohexene.
[c] C.O. = cracking and over oxidation products, O_2/hydroxyl = 0.6.

uct of cyclohexanol, while the SZF catalyst generated mainly cyclohexanone from the oxidization of cyclohexanol. This may be attributed to the existence of more active silver species in the latter catalyst.

Fig. 3 exhibits the conversions and selectivities of aromatic and alicyclic alcohols over the two catalysts. Similar to the aliphatic mono-alcohols, the novel SZF catalyst has higher catalytic activity than the conventional bulk electrolytic silver catalyst, confirming the efficiency of the silver species in the SZF catalyst for alcohol oxidation.

The advantages of the SZF catalyst can be further understood from the analysis of the relationship between the catalytic behavior and the molecular structure of alcohols. For the mono-alcohols, including aliphatic and aromatic alcohols, the improvements in activity are manifested as enhanced conversion, whereas those of the di-alcohols are manifested mainly as enhanced selectivity to the target products. The reason for this could be the different structures of the reactants. For the mono-alcohols, because only one terminal hydroxyl group exists for partial oxidation, the difference between the catalysts is reflected mainly by the conversion as long as the reaction temperature is not high enough to produce overoxidized products (Eq. (1)). For the di-alcohols, because of the existence of the secondary hydroxyl group, a lean oxidation product, α-hydroxyketone, may be generated as a by-product via the oxidation of only one hydroxyl group (Eq. (2)). As a result, the selectivity to the products of moderate oxidation characterizes the improvement in the catalysts if the reaction temperature is not high enough to generate cracking and overoxidized products. As for cyclohexanol, although it is a mono-alcohol, it is somewhat different from its acyclic and aromatic analogues because of its different alcohol hydroxy group (secondary alcohol). Owing to the facile formation of olefin, the oxidation of the hydroxyl to the corresponding carbonyl is comparatively difficult if the activity of catalytic oxidation sites is not high enough, as in the case of bulk electrolytic silver catalyst. Accordingly, its improved selectivity and conversion both contribute to the enhanced catalyst activity.

3.2. Dispersion of silver nanoparticles

Silver nanoparticles are widely used as photosensitive components [15], catalysts [16–20], and agents in surface-enhanced Raman spectroscopy [21–23] because of their special properties. It has been widely accepted that metal particles with an average particle size <100 nm have a high surface area and a high fraction of atoms located on their surfaces, which give high catalytic activity [24]. One of the reasons for the extraordinary catalytic behavior of the SZF catalyst compared with the bulk electrolytic silver catalyst may be the existence of abundant silver nanoparticles in the zeolite film.

3.2.1. SEM and TEM

Fig. 4a shows a typical SEM image of the bulk electrolytic silver catalyst at a magnification of 500×. This image illustrates

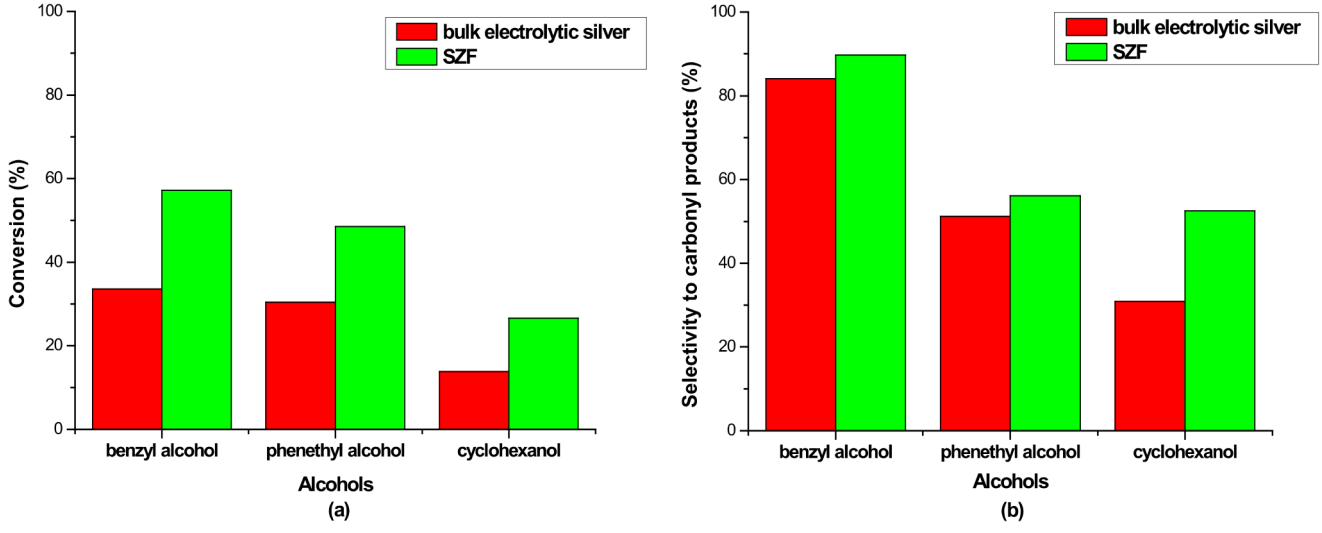

Fig. 3. Comparison of the conversion (a) and selectivity to carbonyl products (b) in the selective oxidation of various aromatic and alicyclic alcohols over the SZF and the bulk electrolytic silver catalysts at 320 °C. O_2/hydroxyl = 0.6, LHSV of the SZF catalyst = 50 h^{-1}, LHSV of the bulk electrolytic silver catalyst = 4 h^{-1}.

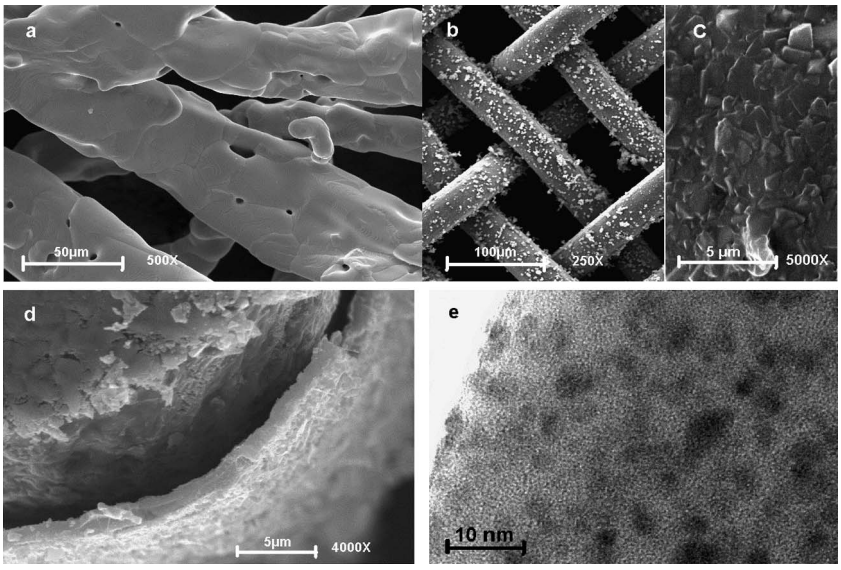

Fig. 4. SEM images of the bulk electrolytic silver catalyst (a), the ZFC (b), the zeolite film of ZFC at high magnification (c), and the SZF catalyst after calcinations (d); TEM image of the SZF catalyst after calcinations (e).

that the bulk electrolytic silver particles easily form a large macroscopic structure larger than 100 μm. Fig. 4b exhibits the gird structure of the prepared ZFC, the surface of which is covered by a compacted zeolite film of 1 μm zeolite crystal (Fig. 4c) with a thickness of ca. 1 μm (cf. Fig. 4d). Electrochemically treating the ZFC in the $AgNO_3$ solution, followed by calcination at 400 °C, yielded a catalyst with highly dispersed silver nanoparticles (Figs. 4d and 4e). The silver nanoparticles are predominately 2–3 nm in size, although a few larger ones are seen (Fig. 4e). The high and stable dispersion of silver nanoparticles may be attributed to the strong hindering effect from the zeolite film against the agglomeration of metal nanoparticles, which leads to high activity for alcohol oxidation [12,13]. The zeolite film has two advantages in the production of in situ electrolytic silver nanoparticles. First, the enriched and uniform micropore channels in zeolite film provide ideal electrolytic tunnels for in situ electrolysis of Ag^+ ions, which may benefit the subsequent formation of highly dispersed silver nanoparticles. Second, the intact zeolite film with sufficient mechanical strength will maintain a smooth and homogeneous electrolytic process, whereas a damaged film will cause the partial agglomeration of silver particles.

3.2.2. XRD and elemental analysis

The XRD patterns of the SZF catalyst and the bulk electrolytic silver catalyst after calcination at 400 °C for 2 h are displayed in Fig. 5. It is obvious that the Ag in the SZF catalyst exists mainly as metallic silver after calcination. The diffraction peaks of the zeolite film are indistinguishable in the XRD pattern, probably due to thinness of the zeolite film on the Cu grids, as indicated on SEM (ca. 1 μm; Fig. 4). An ultra-thin zeolite film is expected because it would not influence the heat conductivity of the catalyst, which is of great significance for industrial applications, especially for the exothermal oxidation reaction.

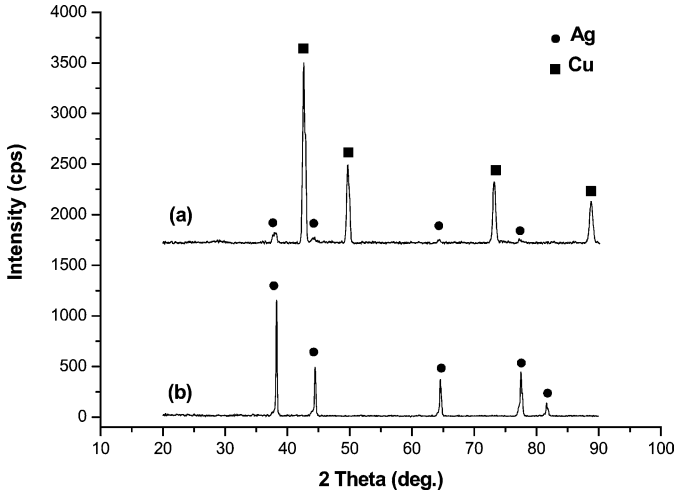

Fig. 5. XRD patterns of the SZF catalyst (a) and the bulk electrolytic silver catalyst (b) after being calcined at 400 °C for 2 h.

3.2.3. TG–DTA analysis

Within the studied temperature range (room temperature to 800 °C), no evident changes were observed in the DTA and TG curves of the two catalysts, indicating that the SZF catalyst is stable at least up to 800 °C as bulk electrolytic silver, although the former is composed of nanosized silver particles that theoretically have a high tendency to sinter. These thermoanalysis results again indicate the effectiveness of the hindering effect of zeolite film against the sintering of the silver nanoparticles, in accordance with the SEM and TEM findings. Such a thermal stability of the SZF catalyst is of importance for the alcohol oxidation reaction.

3.3. Active sites

The electronic properties of the silver catalysts play a major role in the selective oxidation of alcohols [25]. Pestryakov

and Davydov pointed out that for catalysts based on the Cu subgroup, which have been widely used in the oxidation processes of alcohols, the M^+ cations with a maximal effective charge are the active sites [26]. Here the effective charge of the Ag ions in the SZF catalyst was investigated by UV–vis DRS and XPS to explain its high activity in the selective oxidation of alcohols.

3.3.1. UV–vis DRS

The UV–vis DRS technique is a very useful tool for investigating the state of silver particles in catalysts [27,28]. Fig. 6a, b, and d illustrate the UV–vis DRS spectra of the SZF, ZFC, and bulk electrolytic silver catalysts, respectively. For the sake of comparison, Fig. 6c shows the silver spectrum of the SZF catalyst deducted by the spectrum of ZFC. The absorption band at 310–315 nm is commonly ascribed to metallic silver particles or silver foil (intrinsic photo effect), whereas those at 240–250 nm and 270–290 nm are assigned to Ag^+ ions ($s-p$, $d-p$ electron transitions) and charged $Ag_n^{\delta+}$ clusters, respectively [29–31]. The bulk electrolytic silver catalyst displays a sharp and dominant peak centered at 315 nm, indicating the existence of a large amount of metallic silver film and large particles. In the case of the SZF catalyst, however, the peak at 315 nm is dramatically weakened, and the peak between 250 and 300 nm becomes predominant, indicating that nanosized silver particles in this catalyst are composed of much more isolated Ag^+ ions and/or $Ag_n^{\delta+}$ clusters.

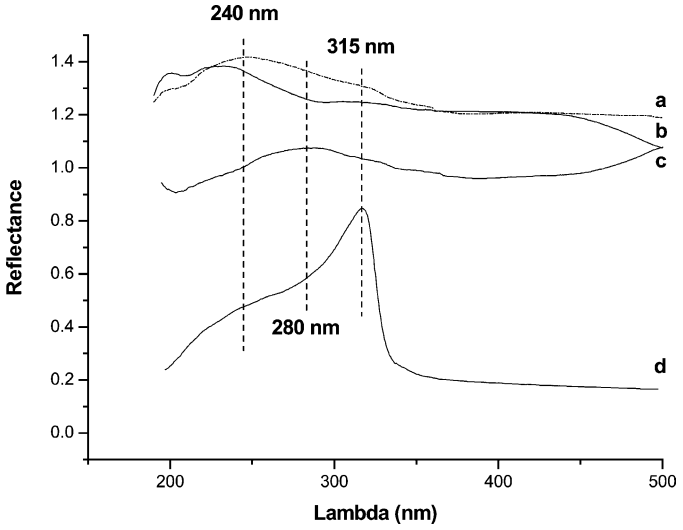

Fig. 6. UV–vis DRS spectra of the SZF catalyst (a), the ZFC (b), difference spectrum of silver nanoparticles obtained by subtracting ZFC contribution from the SZF catalyst spectrum (c) and the bulk electrolytic silver catalyst (d) after calcination at 400 °C for 2 h.

3.3.2. XPS

XPS can provide further information on the chemical state of silver in the catalysts [32,33] by the shift of the Ag $3d_{5/2}$ peak (Fig. 7). The binding energies (BEs) of the Ag $3d_{5/2}$ peak for the SZF catalyst and for bulk electrolytic silver were 367.6 and 367.2 eV, respectively. The positive BE shift of the Ag $3d_{5/2}$ peak of SZF catalyst compared with that of bulk electrolytic silver indicates the existence of more silver ions with positive charge on the silver surface of the SZF catalyst, because the lower electron density in cations compared to that of the metal atoms would reduce the screening of the core-level electrons from their nucleus. Furthermore, the higher BE indicates the greater stability of the Ag^+ ions and $Ag_n^{\delta+}$ clusters in SZF. These results are consistent with those derived from the UV–vis DRS spectra.

As the active sites for the selective oxidation of alcohols [8,25], the stable existence of a large amount of Ag^+ ions and $Ag_n^{\delta+}$ clusters in SZF could well explain its high activity for the mono-alcohol and the high selectivity to moderately oxidized products derived from the di-alcohol. On the other hand, the enhanced silver activity at lower temperatures makes it unnecessary to react in the high-temperature range as in the case

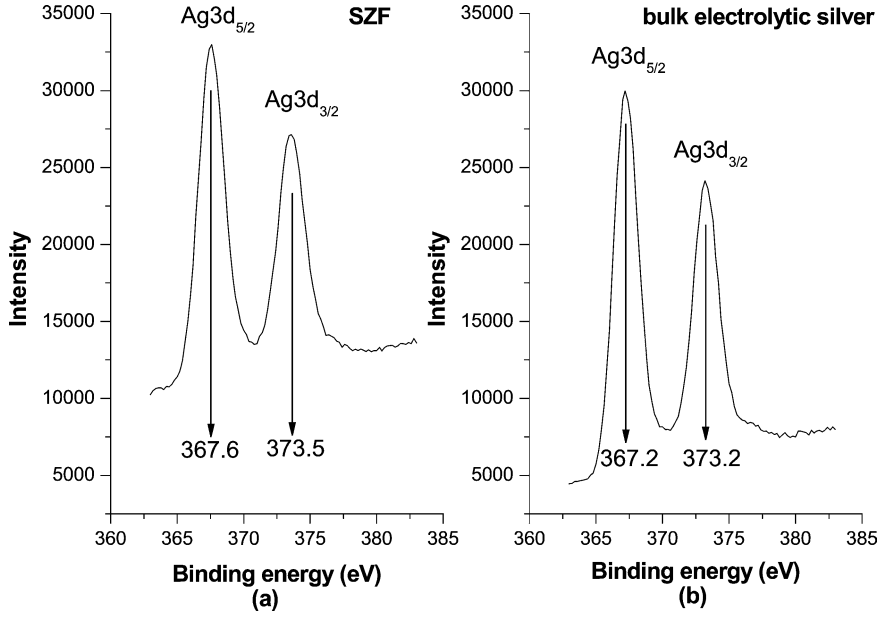

Fig. 7. XPS Ag $3d$ spectra of (a) the SZF catalysts and (b) the bulk electrolytic silver catalyst.

of conventional bulk electrolytic silver, which may successfully prevent the production of cracking and overoxidized products.

4. Conclusion

A novel silver catalyst (SZF) with high alcohol oxidation activity was synthesized by in situ electrolysis of silver nanoparticles on ZFC. Because of the existence of a large amount of highly-dispersed silver nanoparticles and an accordingly abundant number of active sites (Ag^+ ions and $Ag_n^{\delta+}$ clusters) on silver nanoparticles, the SZF catalyst has excellent catalytic oxidation properties in the selective oxidation of mono-alcohols, di-alcohols, and other types of alcohols via significant enhancement of activity and/or selectivity to the target products. The high activity results in a dramatic lowering of the optimal reaction temperature and, accordingly, the prevention of cracking and overoxidation. In addition, the ultra-thin zeolite film-coated copper substrate of the catalyst provides high heat conductivity, which benefits the strong exothermic oxidation reactions.

Acknowledgments

Financial support was provided by the NSFC (grants 20421303, 20473022, 20325313, 20233030, and 20273016), the STCSM (grants 03DJ14004 and 05XD14002), the Ministry of Education (grant 104076), and the Major State Basic Research Development Program (grant 2003CB615807).

References

[1] J. Shen, W. Shan, Y.-H. Zhang, J.-M. Du, H.-L. Xu, K.-N. Fan, W. Shen, Y. Tang, Chem. Commun. 24 (2004) 2880.
[2] R.P. Unnikrishnan, S.-D. Endalkachew, J. Catal. 211 (2002) 434.
[3] R.A. Sheldon, J.K. Kochi, Metal-Catalyzed Oxidation of Organic Compounds, Academic Press, New York, 1981.
[4] M. Qian, M.A. Liauw, G. Emig, Appl. Catal. A 238 (2003) 211.
[5] B.M. Abu-Zied, Appl. Catal. A 198 (2000) 147.
[6] O.V. Vodyankina, S.V. Koscheev, V.T. Yakushko, A.N. Salanov, A.I. Boronin, L.N. Kurina, J. Mol. Catal. A 158 (2000) 381.
[7] W.-L. Dai, Q. Liu, Y. Cao, J.-F. Deng, Appl. Catal. A 175 (1998) 83.
[8] A.N. Pestryakov, Catal. Today 28 (1996) 239.
[9] W.-L. Dai, Y. Cao, L.-P. Ren, X.-L. Yang, J.-H. Xu, H.-X. Li, H.-Y. He, K.-N. Fan, J. Catal. 228 (2004) 80.
[10] M.V. Twigg, Catalyst Handbook, Wolfe, London, 1989, p. 490.
[11] A.N. Pestryakov, N.E. Bogdanchikova, A. Knop-Gericke, Catal. Today 91–92 (2004) 49.
[12] Y.H. Zhang, F. Chen, J.H. Zhuang, Y. Tang, D.J. Wang, Y.J. Wang, A.G. Dong, N. Ren, Chem. Commun. (2002) 2814.
[13] T.V. Choudhary, C. Sivadinazayana, C.C. Chusuei, A.K. Datye, J.P. Fackler, D.W. Goodman, J. Catal. 207 (2002) 247.
[14] I. Kumakiri, T. Yamaguchi, S. Nakao, Ind. Eng. Chem. Res. 38 (1999) 4682.
[15] R.K. Hailstone, J. Phys. Chem. 99 (1995) 4414.
[16] H. Tada, K. Teranishi, Y. Inubushi, S. Ito, Langmuir 16 (2000) 3304.
[17] H. Tada, K. Teranishi, S. Ito, Langmuir 15 (1999) 7084.
[18] A. Sclafani, J. Herrmann, J. Photochem. Photobiol. A 113 (1998) 181.
[19] T. Sun, K. Seff, Chem. Rev. 94 (1994) 857.
[20] P. Claus, H. Hofmeister, J. Phys. Chem. B 103 (1999) 2766.
[21] N. Shirtcliffe, U. Nickel, S. Schneider, J. Colloid Interface Sci. 211 (1999) 122.
[22] U. Nickel, A. zu Castell, K. Pöppl, S. Schneider, Langmuir 16 (2000) 9087.
[23] R.M. Bright, M.D. Musick, M.J. Natan, Langmuir 14 (1998) 5695.
[24] I.T.H. Chang, Z. Ren, Mater. Sci. Eng. A 375–377 (2004) 66.
[25] A.N. Pestryakov, A.A. Davydov, Appl. Catal. A 120 (1994) 12.
[26] A.N. Pestryakov, V.V. Lunin, J. Mol. Catal. A 158 (2000) 329.
[27] W.N. Delgass, Spectroscopy in Heterogeneous Catalysis, Academic Press, New York, 1979, p. 86, chap. 4.
[28] L.R. Gellens, R.A. Schoonheydt, in: P.A. Jacobs (Ed.), Metal Microstructure in Zeolites, Elsevier, Amsterdam, 1982, p. 87.
[29] A.N. Pestryakov, A.A. Davydov, L.N. Kurina, J. Phys. Chem. 60 (1986) 2081 (in Russian).
[30] S.P. Noskova, A.A. Davydov, A.N. Pestryakov, J. Appl. Chem. 61 (1988) 2021 (in Russian).
[31] H.E. Rhodes, P.-K. Wang, H.T. Stokes, C.P. Slichter, J.H. Sinfelt, Phys. Rev. 1326 (1982) 3569.
[32] T. Ishizaka, S. Muto, Y. Kurokawa, Optics Commun. 190 (2001) 388.
[33] J.T. Wolan, G.B. Hoflund, Appl. Surf. Sci. 125 (1998) 251.